RSC Pharmaceutics

Accepted Manuscript

This article can be cited before page numbers have been issued, to do this please use: C. Chevaleyre, S. Tran, M. Richard, L. Jourdain, D. kereselidze, B. Jego, E. Selingue, B. Larrat, S. Mériaux, N. Tournier, A. Novell and C. Truillet, *RSC Pharm.*, 2025, DOI: 10.1039/D5PM00088B.

Reversibility of FUS-aided blood-tumor barrier opening for the delivery of therapeutics.

View Article Online
DOI: 10.1039/D5PM00088B

Céline Chevaleyre[1], Sophie Tran[1], Mylène Richard[1], Laurène Jourdain[1], Dimitri Kereselidze[1], Benoit Jego[1], Erwan Selingue[2], Benoit Larrat[2], Sébastien Mériaux[2], Nicolas Tournier[1], Anthony Novell[1,*], Charles Truillet[1,*].

[1]Paris-Saclay University, CEA, CNRS, Inserm, BioMaps, Service Hospitalier Frédéric Joliot, Orsay France.

[2]Paris-Saclay University, CEA, CNRS, NeuroSpin/BAOBAB, Centre d'études de Saclay, Bâtiment 145, 91191 Gif sur Yvette, France.

Corresponding authors

Anthony Novell, PhD.

SHFJ, 4 place du Général Leclerc, 91401 Orsay, France.

anthony.novell@universite-paris-saclay.fr;

Charles Truillet, PhD.

SHFJ, 4 place du Général Leclerc, 91401 Orsay, France.

charles.truillet@cea.fr

First Author

Céline Chevaleyre, PharmD, PhD student

SHFJ, 4 place du Général Leclerc, 91401 Orsay, France.

celine.chevaleyre@universite-paris-saclay.fr

View Article Online
DOI: 10.1039/D5PM00088B

Abstract

Focused ultrasound (FUS) offers reversible disruption of the blood-brain barrier (BBB), which enables drug delivery to the brain. However, the impact of FUS on the blood-tumor barrier (BTB) remains largely misunderstood. The reversibility of FUS-induced BTB opening was monitored using PET imaging in a glioblastoma model. C57Bl/6 mice with bilateral GL261-GFP tumors received FUS specifically targeting the right hemisphere, followed by injections of the BBB permeability marker [^{18}F]Fluoro-deoxysorbitol (183 Da) or the radiolabeled antibody [^{18}F]avelumab (150 kDa). PET acquisitions were performed after 1h, 24h and 72h post-FUS. The uptake of [^{18}F]avelumab and [^{18}F]Fluoro-deoxysorbitol was increased immediately after FUS. At 24h post-FUS, BTB permeability returned to baseline as evidenced by consistent [^{18}F]avelumab distribution volumes (V_T) between tumors. By 72h, increased radiotracer uptake indicated tumor progression. These findings highlight the potential of FUS to enhance the brain delivery of therapeutics while preserving the BTB integrity over time.

Keywords: Glioblastoma**,** BTB, FUS opening, ImmunoPET imaging, immunotherapy

INTRODUCTION

The vasculature within gliomas is dysfunctional, comprising a mix of continuous capillaries, fenestrated capillaries, and capillaries with inter-endothelial gaps (*1*). This distinct vascular network is referred to as the blood-tumor barrier (BTB), a critical component of glioma biology. Despite its enhanced permeability compared to the blood-brain barrier (BBB) a high selective barrier composed of endothelial cells, pericytes, and astrocytes, the BTB remains a significant obstacle to effective drug delivery to glioma tissues. While BBB protects the brain by limiting substance passage from the bloodstream, the BTB forms when brain tumors disrupt the BBB, creating a more permeable but heterogeneous vasculature. This results in abnormal blood vessels, damaged endothelial cells, and disrupted tight junctions, causing uneven drug delivery and treatment efficacy within tumors. Despite being leakier than the BBB, the BTB still hinders many chemotherapeutic agents, with permeability varying across tumor types and regions (*2*). This variability in drug delivery poses a major challenge for the consistency of therapeutic efficacy in patients (*3*).

One promising technique to address this issue is focused ultrasound (FUS)-mediated brain barrier opening (*4*). This non-invasive approach has been extensively studied and applied to enhance the delivery of chemotherapy and immunotherapy directly to glioma tissues. FUS applied on intravenously administered microbubbles temporarily disrupts the BBB and BTB, allowing greater penetration of therapeutic agents, and could boost antitumor immune responses in patients with high-grade gliomas (*5*). Remarkably, the safety of this method has been widely demonstrated in humans (*6*), making it an attractive option for glioma treatment.

While FUS-aided BBB disruption has been widely studied, including by our research team (*7–9*), the specific effects of FUS on the BTB remain underexplored. In particular, the transient nature of FUS-mediated BTB disruption needs further investigation, given the delicate structure of the BTB and its link with tumor progression.

In this study, we aim to quantitatively investigate the effects of FUS on the BTB by employing positron emission tomography (PET). The BTB's status was monitored post-FUS by tracking the passage of both a large biomolecule, [^{18}F]avelumab (150 kDa), and a small molecule [^{18}F]Fluoro-deoxysorbitol ([^{18}F]FDS, 183 Da), a marker of BBB permeability, across the barrier at selected time points.

MATERIALS AND METHODS

The detailed method is available in the supplementary.

View Article Online
DOI: 10.1039/D5PM00088B

GL261-GFP orthotopic model. Eight C57BL/6 mice were orthotopically implanted with the syngeneic cell line GL261-GFP (obtained from the Institute of Neurophysiopathology, Aix-Marseille University), 5.10^4 cells in 1 µL PBS into both striata. With bregma as origin, implantations coordinates were X= 0mm, Y=±2mm, Z=-3mm. We achieved a 100% tumor formation success rate post-implantation, confirmed by MRI.

MRI Fourteen days after GL261-GFP implantation, T1-weighted contrast-enhanced MRI were acquired with a 7T/90mm bore hole MRI scanner (Pharmascan scanner, Bruker). A Gadolinium-based contrast agent (Dotarem®, 1nm diameter, 100 µL by animal) was intravenously injected via a catheter before acquiring T1-weighted images.

Radiolabeling of the avelumab. Radiofluorination of [^{18}F]avelumab was carried out in two steps. Prosthetic group [^{18}F]FPyNHS was first synthesized on an AllInOne automate (*10*) and then conjugated to avelumab via the amino group of lysine residues.

[^{18}F]FDS production. [^{18}F]FDS was obtained according to a previously protocol (*11*).

Blood-tumor barrier disruption. The FUS protocol was similar to that used in (*8*), except that ultrasound was transmitted in only one hemisphere. This FUS condition has been already demonstrated to be safe (*12*). Briefly, 50 µL of SonoVue microbubbles (Bracco) were intravenously administered before the sonication. A large mechanical scan of 6 mm × 6 mm was performed over the animal's head, but ultrasound (1.5 MHz, 420 kPa) was only transmitted over a 6 mm × 3.6 mm area corresponding to the right hemisphere only, enabling the BBB disruption to the full depth of the brain hemisphere. Acoustic pressure was set at 0 kPa over the rest of the trajectory, allowing the left hemisphere to remain as a control. The trajectory was repeated for a total of 2 min.

microPET/CT imaging. On day 15 after GL261-GFP implantation, a 60-min dynamic PET scan was performed after injection of [^{18}F]avelumab (6.7±4.2MBq, 75±4µg, n=4) under camera,. A 30-min dynamic PET scan was performed after injection of [^{18}F]avelumab (6.7±1.7MBq, n=4) under camera. The radioligand injection was performed immediately after the end of the FUS protocol, 2.9±0.1 min for the [^{18}F]avelumab and 2.9±0.0min for the [^{18}F]FDS. Subsequent [^{18}F]avelumab PET scans were performed at 24h (9.5±4.5MBq, 80±6µg, n=4) and 72h post-FUS (3.7±1.8MBq, 62±2µg, n=4). Subsequent [^{18}F]FDS PET scans were performed at 24h (7.7±4.2MBq, n=4) and 72h post-FUS (10.2±1.3MBq, n=4).

Immunofluorescence After the last imaging session, mice were sacrificed and perfused with saline solution. Their brains were collected, immersed in isopentane, and frozen in liquid nitrogen. A set of fixed frozen brain sections (10 µm) was incubated with an anti-GFP AF488 and rat anti-mouse CD31 antibodies. The slides were then incubated with an anti-rat AF546-conjugated secondary antibody and an AF647-conjugated goat anti-human secondary antibody to stain the injected avelumab. Immunofluorescent sections were scanned with AxiObserver Z1 microscope (Zeiss).

RESULTS

Distribution of [^{18}F]avelumab and [^{18}F]FDS following BTB disruption by FUS.

As anticipated, the BTB in the GL261-GFP model showed some leakage, allowing both [^{18}F]avelumab and [^{18}F]FDS to cross into the left tumor which did not receive FUS (Figure 1B). After FUS treatment on the right hemisphere, [^{18}F]avelumab uptake in the right tumor was slightly higher compared to the left tumor ($AUC_{0\text{-}60min}$= 161±9 versus 143±8 %ID.min.cm^{-3}, $p<0.01$, Figure S7). For [^{18}F]FDS, there was no significant difference in exposure between the right and left tumors ($AUC_{0\text{-}30}$= 44±3 in the left tumor and 45±2 %ID.min.cm^{-3} in the right tumor, $p>0.05$, Figure S8). At 24 and 72 hours post-FUS, the left tumor, which did not receive FUS, showed higher exposure to both radioligands. This is consistent with the initial BTB status observed in the T1-weighted contrast-enhanced MRI where the left tumor present

View Article Online
DOI: 10.1039/D5PM00088B

higher volume than the right tumor (Figure S6-8). As a consequence, the FUS-to-sham tumor ratio of [^{18}F]avelumab was greater immediately after FUS, but not at 24 and 72 hours post-FUS, where the ratio remained stable (1.25±0.27 at 1h post-FUS, versus 0.85±0.13; $p<0.01$ at 24h and 0.89±0.07; p-value =0.04 at 72h) (Figure 1D-E). [^{18}F]avelumab blood pool content was significantly higher at 24 hours, that can be explained by a saturation of the antigen sink between 24h-48h related to the long half-life of avelumab.

Quantifying the passage of [^{18}F]-avelumab provides insights into the BTB status.

The distribution volume ($V_T = K_1/k_2$) of [^{18}F]avelumab was estimated by fitting a 1-tissue compartment model to the tumors' time-activity curves. Immediately following FUS-aided disruption, the V_T in targeted tumors increased significantly by ~50%. Interestingly, 24 hours later, the V_T in FUS-treated tumors dropped sharply, falling below the levels observed in the sham-treated tumors. At 72 hours, V_T increased in all tumors, with higher values remaining in the sham-treated tumors (Figure 2A). No significant correlation was observed between the V_T obtained 1h post-FUS and tumor volume determined on MRI. In contrast, a significant correlation emerged 24 hours later between V_T and the baseline BTB status (before FUS, Figure 2B). This suggests that 24 hours post-FUS, the observed uptake in the tumor is more closely related to the tumor burden. In contrast, the increased uptake immediately after FUS is likely due to enhanced drug entry into the tumor (Figure S9-10). Immunofluorescence analysis at 72 hours post-FUS revealed that the total amount of avelumab in the FUS-treated tumor was significantly higher than in the sham tumor (Figure 2C, with quantification in Figure S11). This underscores the critical role of FUS in enhancing avelumab delivery in a reversible manner, compared to its natural passage through the impaired BTB.

DISCUSSION/CONCLUSION

It is generally accepted that BBB disruption after FUS is reversible, within 24 hours, a conclusion largely based on preclinical and clinical studies using gadolinium-based MRI contrast agents in the context of a healthy and functional BBB (*6*). In clinical trials evaluating the treatment of brain tumors by FUS-enhanced delivery of therapeutics, the targeted lesions already dispose of a dysfunctional BTB that allows the diffusion of MRI contrast agent before any FUS (*13*). Given that the BTB is inherently fragile and exhibits heterogeneous vascular structures,(*14*) the transient nature of FUS-induced disruption required further investigation.

In a recent study, we assessed the extent and duration of BBB and BTB opening for a full IgG antibody following FUS exposure, with both being comparable (*8*). However, when monitoring the kinetics of the radiolabeled antibody, we observed a progressive accumulation in the tumor beginning 48 hours post-injection, following FUS-induced BBB/BTB opening. Based on these findings, it remains unclear whether this accumulation is due to the tumor's natural progression or a prolonged effect of the FUS on the BTB.

The present study demonstrates that the delivery of [^{18}F]avelumab is facilitated by the FUS-induced BTB opening, but less profitable for the [^{18}F]FDS explained by its smaller molecular weight and rapid plasma clearance compared to a full IgG such as avelumab. As vascular endothelium reclosure after FUS is progressive, the time during which paracellular passage is possible is highly dependent on the size and physicochemical properties of the therapeutic molecule under consideration (*7*,*15*). Furthermore, it is recognized that the opening of the BBB by FUS induces inflammatory reactions and regulates the expression of certain proteins, effects that may persist for several days (*16*,*17*). Therefore, size is an important but not the only parameter of the tumor uptake of a drug. BTB is characterized by a decreased expression of influx and efflux transporters accompanied by an increase in the number of caveolae and an intensification of pinocytosis (*18*). Recent studies suggest that the distribution of therapeutic antibodies in brain metastases may rely more on active intracellular transport mechanisms,

View Article Online
DOI: 10.1039/D5PM00088B

such as endocytosis, rather than solely on paracellular permeability (*19*,*20*). This highlights the complex relationship between BTB dynamics and molecular size, where larger molecules like antibodies can, in some cases, achieve greater efficacy than smaller compounds. FUS may not only facilitate paracellular transport but also modulate intracellular trafficking pathways at the BTB, potentially enhancing the delivery of larger molecules. This additional layer of complexity in BTB modulation by FUS should be further explored to fully leverage its therapeutic potential for brain tumors.

However, at 24 hours post-FUS, the BTB's permeability returned to baseline levels comparable to those obtained before FUS. By 72 hours post-FUS, the increased distribution of both [^{18}F]avelumab and [^{18}F]FDS across all tumors suggests tumor progression consistent with the aggressive nature of the GL261-GFP glioblastoma model, with progressive increase in BTB permeability. Additionally, quantification of the TRICT-dextran injected 72h post-FUS showed no significant difference between the two tumors, further confirming the reversibility of the FUS-induced BTB disruption (Figure S12). This finding underscores the need for multiple FUS sessions to optimize drug delivery, even when the BTB is already leaky, to reinforce the potential of therapeutics for improved and/or homogeneous treatment outcomes. The necessity for repeated FUS treatments may vary depending on the tumor type and its specific characteristics in clinical practices. For instance, tumors with inherently leaky BTBs might require several FUS sessions but fewer compared to those with more intact barriers to reach an optimal drug occupancy. Personalized treatment strategies, tailored to the individual characteristics of each patient's tumor, are likely required to maximize therapeutic efficacy. Such strategies could involve adjusting the frequency and timing of FUS sessions based on real-time monitoring of BTB permeability and tumor response.

Disclosure.

AN&BL is stockholder of a company developing a FUS device for BBB opening in patients. Other authors have no relevant financial or non-financial interests to disclose.

Funding.

We gratefully acknowledge the financial support from ITMO Cancer-Aviesan, provided through INSERM for the IM2FUS project and from INCA – High Risk High Gain for the Keystone project. This work was conducted using an imaging platform that is part of the France Life Imaging network (grant ANR-11-INBS-0006).

Author Contributions statement

Conception and design: CC, AN, CT / analysis and interpretation of the data: CC, ST, MR, LJ, DK, BJ, ES, BL, SM, NT, AN, CT / Drafting of the paper: CC, MR, NT, AN, CT / revising it critically for intellectual content: CC, ST, MR, LJ, DK, BJ, ES, BL, SM, NT, AN, CT / the final approval of the version to be published: CC, ST, MR, LJ, DK, BJ, ES, BL, SM, NT, AN, CT. All authors agree to be accountable for all aspects of the work.

Data Availability Statement

All data supporting this study is included in the article and supporting information.

Animals.

The authors have adhered to the ARRIVE guidelines. There is no fully reliable or validated alternative to animal models for reproducing the intricate complexity of the tumor microenvironment, particularly the unique vascularization seen in glioblastoma. While in vitro systems, such as cell lines or organoids, and in silico simulations enable the study of isolated mechanisms, they fall short of capturing the dynamic interplay between immune cells, metabolic pathways, and vascular networks within a living organism. Animal experiments were conducted on six-week-old female C57BL/6 NRj mice (Janvier

View Article Online
DOI: 10.1039/D5PM00088B

Labs) in accordance with European Directive 2010/63/EU and its transposition into French law (Decree No. 2013-118). The study was approved by a local ethics committee and carried out at the CEA-SHFJ imaging platform (authorization D91–471-105). Mice were housed in standard conditions: microisolator polycarbonate cages with aspen wood bedding, five animals per cage, at a controlled room temperature of 22°C and 40% humidity under a 12-hour light/dark cycle. Food and water were provided ad libitum. During imaging, anesthesia was induced and maintained with isoflurane (2% to 2.5%) in an oxygen flow. To prevent hypothermia, animals were placed on a heated platform, maintaining their body temperature between 36°C and 37°C. The animals were humanely euthanized via cervical dislocation under deep anesthesia induced by 4% isoflurane. This method ensures rapid and ethically compliant termination, minimizing any potential suffering.

REFERENCES

1. Upton DH, Ung C, George SM, Tsoli M, Kavallaris M, Ziegler DS. Challenges and opportunities to penetrate the blood-brain barrier for brain cancer therapy. *Theranostics*. 2022;12:4734-4752.

2. Pinkiewicz M, Pinkiewicz M, Walecki J, Zaczyński A, Zawadzki M. Breaking Barriers in Neuro-Oncology: A Scoping Literature Review on Invasive and Non-Invasive Techniques for Blood-Brain Barrier Disruption. *Cancers*. 2024;16:236.

3. Arvanitis CD, Ferraro GB, Jain RK. The blood-brain barrier and blood-tumour barrier in brain tumours and metastases. *Nat Rev Cancer*. 2020;20:26-41.

4. Bérard C, Truillet C, Larrat B, et al. Anticancer drug delivery by focused ultrasound-mediated blood-brain/tumor barrier disruption for glioma therapy: From benchside to bedside. *Pharmacol Ther*. 2023;250:108518.

5. Cohen-Inbar O, Xu Z, Sheehan JP. Focused ultrasound-aided immunomodulation in glioblastoma multiforme: a therapeutic concept. *J Ther Ultrasound*. 2016;4:2.

6. Mainprize T, Lipsman N, Huang Y, et al. Blood-Brain Barrier Opening in Primary Brain Tumors with Non-invasive MR-Guided Focused Ultrasound: A Clinical Safety and Feasibility Study. *Sci Rep*. 2019;9:321.

7. Marty B, Larrat B, Van Landeghem M, et al. Dynamic study of blood-brain barrier closure after its disruption using ultrasound: a quantitative analysis. *J Cereb Blood Flow Metab Off J Int Soc Cereb Blood Flow Metab*. 2012;32:1948-1958.

8. Chevaleyre C, Novell A, Tournier N, et al. Efficient PD-L1 imaging of murine glioblastoma with FUS-aided immunoPET by leveraging FcRn-antibody interaction. *Theranostics*. 2023;13:5584-5596.

9. Tran VL, Novell A, Tournier N, et al. Impact of blood-brain barrier permeabilization induced by ultrasound associated to microbubbles on the brain delivery and kinetics of cetuximab: An immunoPET study using 89Zr-cetuximab. *J Controlled Release*. 2020;328:304-312.

10. Richard M, Specklin S, Roche M, Hinnen F, Kuhnast B. Original synthesis of radiolabeling precursors for batch and on resin one-step/late-stage radiofluorination of peptides. *Chem Commun*. 2020;56:2507-2510.

11. Hugon G, Goutal S, Dauba A, et al. [18F]2-Fluoro-2-deoxy-sorbitol PET Imaging for Quantitative Monitoring of Enhanced Blood-Brain Barrier Permeability Induced by Focused Ultrasound. *Pharmaceutics*. 2021;13:1752.

View Article Online
DOI: 10.1039/D5PM00088B

12. Porret E, Kereselidze D, Dauba A, et al. Refining the delivery and therapeutic efficacy of cetuximab using focused ultrasound in a mouse model of glioblastoma: An 89Zr-cetuximab immunoPET study. *Eur J Pharm Biopharm*. 2023;182:141-151.

13. Meng Y, Reilly RM, Pezo RC, et al. MR-guided focused ultrasound enhances delivery of trastuzumab to Her2-positive brain metastases. *Sci Transl Med*. 2021;13:eabj4011.

14. Dubois LG, Campanati L, Righy C, et al. Gliomas and the vascular fragility of the blood brain barrier. *Front Cell Neurosci*. 2014;8.

15. Arsiwala TA, Blethen KE, Wolford CP, et al. Blood-tumor barrier opening by MRI-guided transcranial focused ultrasound in a preclinical breast cancer brain metastasis model improves efficacy of combinatorial chemotherapy. *Front Oncol*. 2023;13:1104594.

16. Ji R, Karakatsani ME, Burgess M, Smith M, Murillo MF, Konofagou EE. Cavitation modulated inflammatory response following focused ultrasound blood-brain barrier opening. *J Control Release Off J Control Release Soc*. 2021;337:458-471.

17. Goutal S, Novell A, Leterrier S, et al. Imaging the impact of blood-brain barrier disruption induced by focused ultrasound on P-glycoprotein function. *J Controlled Release*. 2023;361:483-492.

18. Pernet-Gallay K, Jouneau P-H, Bertrand A, et al. Vascular permeability in the RG2 glioma model can be mediated by macropinocytosis and be independent of the opening of the tight junction. *J Cereb Blood Flow Metab*. 2017;37:1264-1275.

19. Gril B, Wei D, Zimmer AS, et al. HER2 antibody-drug conjugate controls growth of breast cancer brain metastases in hematogenous xenograft models, with heterogeneous blood–tumor barrier penetration unlinked to a passive marker. *Neuro-Oncol*. 2020;22:1625-1636.

20. Santos L, Moreira JN, Abrunhosa A, Gomes C. Brain metastasis: An insight into novel molecular targets for theranostic approaches. *Crit Rev Oncol Hematol*. 2024;198:104377.

View Article Online
DOI: 10.1039/D5PM00088B

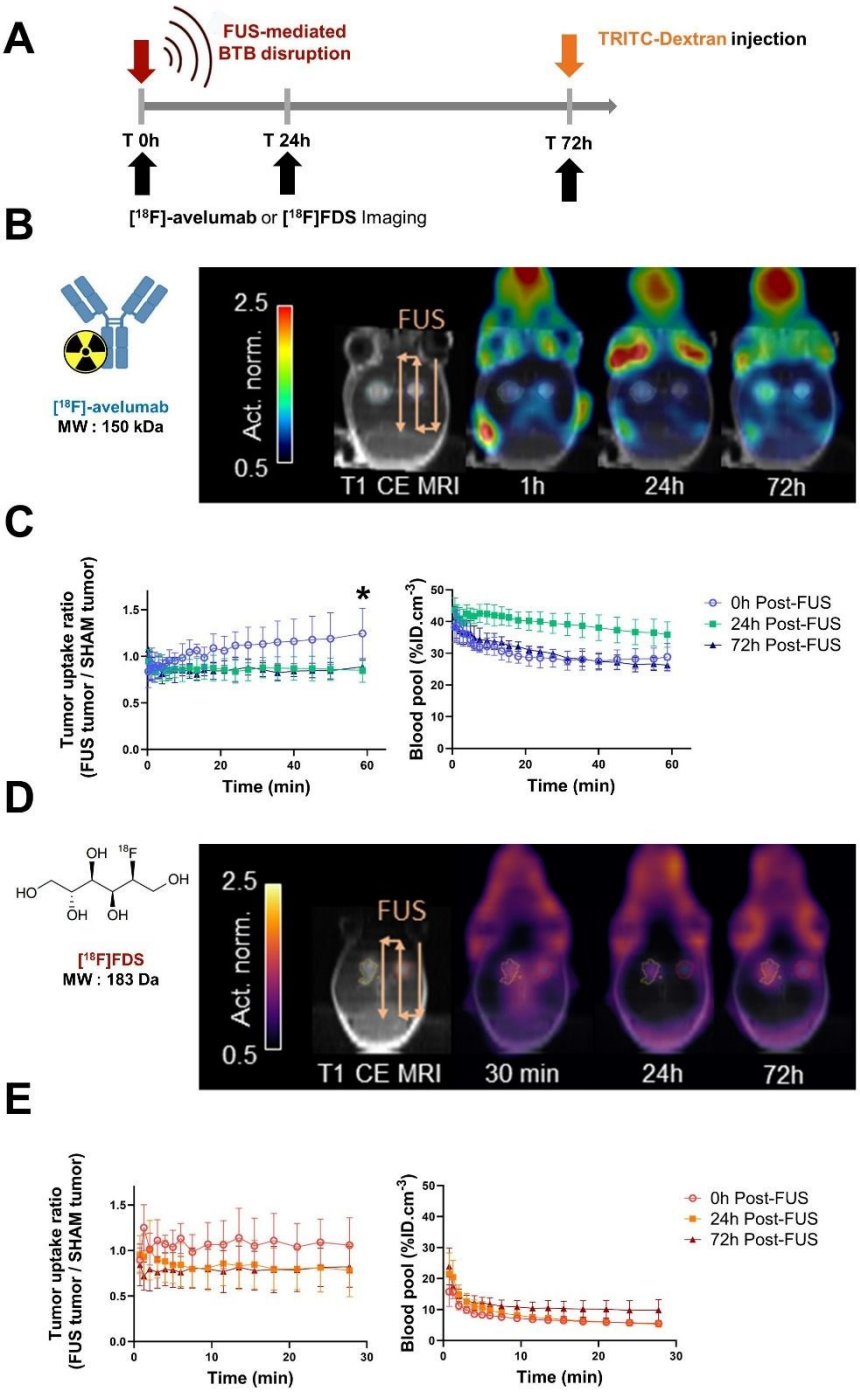

Figure. 1. Blood tumor-barrier opening by FUS and its impact on the delivery of [^{18}F]-avelumab and [^{18}F]FDS. (A) Study timeline. **(B)** Representative T1-weighted MRI with contrast enhancement and averaged PET images on the last 20 minutes of the acquisitions. [^{18}F]-avelumab was injected just after the FUS protocol, 24h and 72h later. PET images are normalized by the peak voxel value in the left tumor. **(C)** Tumor uptake ratios of [^{18}F]-avelumab (n = 4 mice) between the tumor with FUS-aided BTB disruption and the contralateral tumor; corresponding blood curves. **(D)** Representative T1w MRI with contrast enhancement and averaged PET images on the last 10 minutes of the acquisitions. [^{18}F]FDS was injected just avec the FUS protocol, 24h after and 72h after. PET images are normalized by the peak voxel value in the left tumor. **(E)** Tumor uptake ratios of [^{18}F]FDS (n = 4 mice); corresponding blood curves. All data are represented as mean ± SD

View Article Online
DOI: 10.1039/D5PM00088B

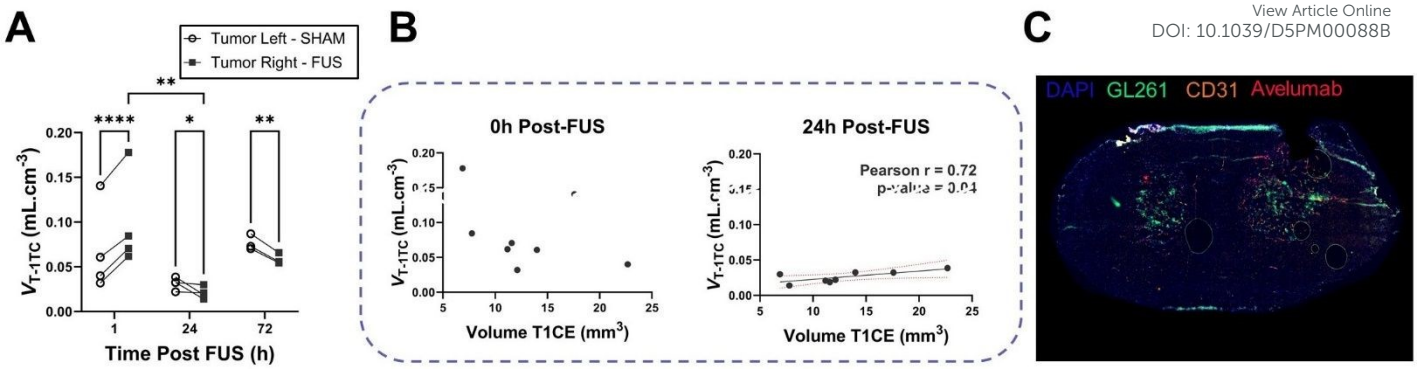

Figure. 2. [^{18}F]-avelumab distribution comparing the disrupt BTB and the sham BTB overtime. **(A)** Distribution volumes (V_T) of [^{18}F]-avelumab estimated from the fitting of a 1-tissue compartment model for the FUS-exposed tumor and the contralateral tumor. **(B)** Correlation between the [^{18}F]-avelumab distribution volume and the volume of the initial BTB disruption determined on the T1-weighted MRI with gadoteric acid contrast enhancement. **(C)** Immunofluorescent staining of the injected avelumab (red) and of the endothelial cells (orange) on a section of a mouse brain bearing two GL261-GFP tumors (green) harvested at 72h post-injection. Immunofluorescence signal is overlaid on DAPI images (blue).

All data supporting this study is included in the article and supporting information.

View Article Online
DOI: 10.1039/D5PM00088B